JOURNAL OF NANO- AND ELECTRONIC PHYSICS
Vol. **18** No 2, 02001(7pp) (2026)

ЖУРНАЛ НАНО- ТА ЕЛЕКТРОННОЇ ФІЗИКИ
Том **18** № 2, 02001(7cc) (2026)

OPEN ACCESS

REGULAR ARTICLE

Growth Kinetics of Ag Clots on AgBr Microcrystals Under the Action of Femtosecond Pulsed Laser Radiation

Oleksandr B. Piven[1,*] ✉, Oleg B. Piven[2,†]

[1] *Cherkasy State Technological University, 18006 Cherkasy, Ukraine*
[2] *National Technical University of Ukraine "Igor Sikorsky Kyiv Polytechnic Institute", 03056 Kyiv, Ukraine*

(Received 01 August 2025; revised manuscript received 18 April 2026; published online 29 April 2026)

Computer modeling revealed the growth kinetics of Ag clots on the surface of AgBr microcrystals of photoemulsion under the action of femtosecond radiation of pulsed lasers of the Flint series (wavelength $\lambda = 1035$ nm, pulse repetition rate $f = 76$ MHz) and FemtoLux 3 series ($\lambda = 1030$ nm, power $P = 3$ W, pulse duration $\tau = 300$ fs). It has been established that the growth time of Ag clots up to a volume $V = 5.23$ m^3, at which its spontaneous crystallization at $T = 300$ K is possible is 1) ~ 10^{-1} s for the FemtoLux 3 series lasers ($f = 1$ MHz, 2 MHz, 3 MHz); 2) ~ 10^{-2} s for Flint 1.0 ($P = 1$ W, $\tau = 80$ fs), Flint 2.0 ($P = 2$ W, $\tau = 100$ fs), Flint 4.0 ($P = 4$ W, $\tau = 100$ fs), Flint 6.0 ($P = 6$ W, $\tau = 100$ fs), Flint 10 ($P = 10$ W, $\tau = 120$ fs) lasers and for of the FemtoLux3 ($f = 4$ MHz, 5 MHz) lasers. This agrees with the fact that no developable Ag particles form at exposure times < s on the surface of AgBr microcrystals.

Keywords: Femtosecond laser irradiation, AgBr microcrystal, Influence of laser radiation, Growth kinetics, Clot of silver, Low-sensitive photolayer, Crystallization.

DOI: 10.21272/jnep.18(2).02001 PACS numbers: 61.46. + w, 61.50.f, 61.80.Ba, 06.60.Jn

1. INTRODUCTION

Femtosecond laser radiation (FLR) is widely used in manufacturing, such as automation technology, information technology, telecommunications technology, biotechnology, pharmaceutical, aerospace, environmental industry [1,2]. Femtosecond lasers (FL) are also used to study ultrafast processes and develop such advanced technologies as time resolved pump-probe shadowgraphy, ultrafast continuous optical imaging, 4-dimensional ultrafast scanning electron microscopy [3]. FLR is used to create new functional materials with controlled optical and electronic characteristics by engineering the semiconductor structure [4].

FLR induces structural changes and electronic excitation of semiconductors [5]. The mechanism of action of FLR, including phase transition and extraction of the material on which this radiation acts, is largely determined by the interaction between laser radiation and electrons [6]. The peculiarity of the FLR action on semiconductor is as follows: FL pulses cause two-/multiphoton excitation on a time scale much faster than the thermal energy exchange between photoexcited electrons and lattice ions [7]. During the FLR action, photons are mainly absorbed by electrons, with subsequent energy transfer from electrons to ions on the order of picoseconds [6]. Therefore, the lattice motion is insignificant during the femtosecond pulse, while the electron-photon interaction dominates throughout the FLR action time [6].

Since the duration of one pulse of a femtosecond laser is within the time frame for chemical reactions (from 10 fs to 100 fs, 1 fs = 10^{-15} s) [8], which includes the reaction of photolysis of an AgBr crystal under the action of light from the absorption region of AgBr.

Silver bromide (AgBr) crystal is a wide-gap ionic semiconductor [9] with a zinc blende structure (face-centered cubic unit cell) with a wide range of technological applications: energy conversion [10], environmental remediation [11], radiation detection [12]. In addition, AgBr crystals have photocatalytic [13], rapid antibacterial and wound repair [14] and anticancer [15] effects.

Silver-based nanocomposites play a key role in material science [16]. The process of formation and properties of Ag clusters on the surface of AgBr crystals under the action of light are also studied [17, 18].

The study of the kinetics of the growth of Ag clusters on the surface of AgBr emulsion microcrystals (MCs) under the action of femtosecond laser pulses can provide more information about ultrafast photoinduced processes in wide-gap semiconductors, about the features of the photographic process on low-sensitivity photolayers. The kinetics of the growth of Ag clusters on the surface of AgBr MCs under the action of laser radiation of continuous-wave and pulsed-wave mode with a duration of radiation pulses greater than a femtosecond for different wavelengths, powers and pulse repetition rates was studied using computer models [19, 20]. These models describe the kinetics of the growth of Ag clusters up to a size of 1 nm, at which these Ag clusters can spontaneously transition to a

* Correspondence e-mail: abpiven@ukr.net
† pivolegbor@gmail.com

Cite this article as: O.B. Piven et al., *J. Nano- Electron. Phys.* 18 No 2, 02001 (2026) https://doi.org/10.21272/jnep.18(2).02001

crystalline state at room temperature [21]. A computer model [22] was created using a two-temperature model [1], molecular dynamics and density functional methods. This model [22] describes the initial stages of the formation of Ag clusters over a time of 10^{-11} s in an AgBr crystal consisting of 32 Ag atoms and 32 Br atoms under the action of FLR.

The authors are not aware of any publications describing the kinetics of the growth of Ag silver clusters up to a size of 1 nm on the surface of AgBr MCs under the action of femtosecond pulsed laser radiation. Therefore, this study is a relevant task.

2. MODELS AND CALCULATION METHODS

Traditionally, the photographic process includes several stages:

1) photogeneration of electron-hole pairs in silver halide crystals;

2) reduction of silver cations to atoms by some part of these electrons;

3) subsequent growth of atoms to obtain clusters (latent image);

4) complete reduction by the developer of crystallites that have more than a critical number of atoms per cluster [23, 24].

Stages 1-3 of the photographic process are described by the system of differential equations (SDE) (8) from [20]. Therefore, to study the kinetics of growth of amorphous Ag clots to sizes at which spontaneous crystallization of these clots is possible at $T = 300$ K, on the surface of AgBr MCs under the action of FLR, this SDE was used.

Let us consider this SDE in more detail. We will consider each silver particle as a sphere of radius R, which grows due to the fluxes of ions and polarized atoms. Under the action of FLR, many growing particles appear in the surface layer of the AgBr microcrystal (MC). Let $2R_m$ be the average distance between the two centers. The attraction of Ag ions and atoms to the growing clot is generated by a flux, the density of which is initially equal to $J_i = n_i \cdot D_i \cdot F_i \cdot (k_b \cdot T)^{-1}$, $J_a = n_a \cdot D_a \cdot F_a \cdot (k_b \cdot T)^{-1}$, where n_i, n_a are the number of stray ions and Ag atoms per unit volume of the microcrystal at $T = 300$ K, D_i, D_a are the diffusion coefficients in the MC of Ag ions and atoms ($D_i = D_a = D$), F_i is the force acting on the ion from the side of the electron that has fixed, F_a is the force of the electron-dipole interaction between the electron that has fixed and the polarized Ag atoms, k_b is the Boltzmann constant. Taking into account that the attraction of the electron fixed at the center to ions and polarized Ag atoms is replaced by a neutralized state of the center, which persists for a certain time until a new electron is captured. Then the force expressions F_i, F_a – must be multiplied by the fraction of the time spent by the particle in the charged state: $F_i = \tau_i \cdot k \cdot e^2/((\tau_i + \tau_e) \cdot R^2)$, $F_a = \alpha \cdot \tau_i \cdot k \cdot e^2/((\tau_i + \tau_e) \cdot R^5)$, where $k = 9*10^9$ m/F, e – the charge of the electron, τ_i – the time until the capture of the Ag ion by the electron fixed in the trap, τ_e – the time until the capture of the emerging electron by the trap, α – the polarizability of the Ag atom. Drift currents on the growing particle cause a redistribution of ions inside the sphere. Therefore, $J_i = -D_i grad(n_i) + n_i \cdot D_i \cdot F_i \cdot (k_b \cdot T)^{-1}$, $J_a = -D_a grad(n_a) + n_a \cdot D_a \cdot F_a \cdot (k_b \cdot T)^{-1}$. The particle growth rate is determined by the mass balance equation

$$\frac{dR}{dt} = -\frac{J_i(t,r) + J_a(t,r)}{n_R}\Big|_{r=R(t)},$$

where n_R is the concentration of atoms in the growing Ag particle.

$$dn_i/dt = \sigma_V - \chi_{ie} \cdot n_i \cdot n_e - 4\pi R^2 |J_i| / \left(4\pi R_m^3 - 4\pi R^2/3\right) \quad (1)$$

The Eq. (1) determines the change in the concentration of Ag^+ ions over time, σ_V is the number of Ag^+ ions or electrons or holes that appeared under the action of laser radiation in a unit volume of the AgBr microcrystal in 1 s. The term – $\chi_{ie}*n_i*n_e$ describes the recombination of Ag^+ ions with mobile electrons during their movement to the traps, forming Ag atoms that have not yet joined the clot. The last term describes the increase in the volume of Ag clots in 1 s due to the addition of Ag atoms formed from electrons fixed on the traps and stray Ag^+ ions. For such a description, the ion flux into a growing clot is divided by the difference between the maximum volume and the clot volume at a given time.

$$dn_a/dt = \sigma_V - \chi_{ie} \cdot n_i \cdot n_e - 4\pi R^2 |J_a| / \left(4\pi R_m^3 - 4\pi R^2/3\right) \quad (2)$$

The Eq. (2) determines the change in the concentration of Ag atoms per unit volume of an AgBr microcrystal per 1 s, which were formed during the recombination of ions and electrons. The first term – $\chi_{ie}*n_i*n_e$ determines that some Ag^+ ions recombine with mobile electrons during their movement to the traps, forming Ag atoms that have not yet joined the clot. The next term describes that some of the Ag atoms are polarized and attracted by the field of the electron that has become fixed, and go to increase the volume of Ag clots per 1 s.

$$dn_e/dt = \sigma_V - \chi_{ie} \cdot n_i \cdot n_e - \chi_{he} \cdot n_h \cdot n_e - n_e/\tau_e \quad (3)$$

The Eq. (3) determines the change in electron concentration. The second term – $\chi_{ie}*n_i*n_e$ determines the recombination of electrons with a part of Ag^+ ions, the third term – $\chi_{he}*n_h*n_e$ determines the recombination of electrons with holes, the last term determines – n_e/τ_e the capture of a part of electrons by traps in 1 s.

$$dn_h/dt = \sigma_V - \chi_{he} \cdot n_h \cdot n_e \quad (4)$$

The Eq. (4) describes the change in the concentration of holes formed under the action of light in a unit volume of an AgBr microcrystal. The term – $\chi_{he} \times n_h \times n_e$ determines the recombination of electrons with holes.

The assumption is made that $\chi_{ie} = \chi_{he}$ where χ_{ie} – describes the recombination frequency of stray Ag^+ ions and electrons, χ_{he} – describes the recombination frequency of stray electrons with holes. Substituting the expressions for J_a, J_i and taking into account the transition from R to V and $4\pi \cdot D \cdot k \cdot e^2 (k_b/T)^{-1}$, $\xi = \chi_{ie}\tau_e$, from Eqs. 1-4 we obtained the system of equations:

$$\begin{cases} dn_i/dt = (\sigma_V(\xi n_h + 1)/(1 + \xi(n_i + n_h))) - (\gamma n_i/(V_m - V)), \\ dn_a/dt = (\sigma_V \xi n_i/(1 + \xi(n_i + n_h))) - (\gamma n_a 4\pi\alpha/(3V(V_m - V))), \\ dn_h/dt = \sigma_V(\xi n_i + 1)/(\xi(n_i + n_h) + 1), \\ dV/dt = (\gamma(n_i + 4\pi\alpha n_a/3V)/n_R). \end{cases} \quad (5)$$

The computer model used Flint series lasers with a beam diameter $d = 1 \times 10^{-3}$ m and FemtoLux3 series lasers with a beam diameter $d = 2 \times 10^{-3}$ m (see Table 1).

For model calculations, the area of the AgBr microcrystal in the photoemulsion SP-1 with sensitivity 6 units GOST was $S = 0.25 \times 10^{-12}$ m^2. Therefore, for model calculations, lasers with different powers, different pulse durations and different pulse repetition frequencies were used (Table 1).

Table 1 – Parameters of femtosecond pulsed lasers (Lithuania-based manufacturers)

Laser number	Laser name	Light wavelength λ (nm)	Laser power (W)	Laser pulse duration $\tau \times 10^{-15}$ s	Pulse repetition rate $f \times 10^6$ s^{-1}
1	Flint 1.0	1035	1	80	76
2	Flint 2.0		2	100	
3	Flint 4.0		4		
4	Flint 6.0		6		
5	Flint 10		10	120	
6	FemtoLux3	1030	3	300	1
7					2
8					3
9					4
10					5

The initial conditions for solving the SDE (5) were as follows: $n_i = 0$, $n_a = 10^{24}$ m^{-3}, $n_h = 0$, $R = 1.44 \times 10^{-10}$ m. The following parameters were calculated in the computer model:

1) the number of quanta N emitted by the laser in 1 s determined by the formula $P = Nh\nu/\eta$ for lasers with $\lambda = 1035$ nm, 1030 nm). Changing $\nu = c/\lambda$ we obtain $N = \eta P\lambda/(hc)$, where h is the Planck constant, c is the speed of light in vacuum, η is the efficiency ($\eta = 0.5$) [20].

2) the area of the laser beam with a diameter of 1×10^{-3} m and 2×10^{-3} m;

3) the area of a conventional microcrystal with a size of 0.5 μm * 0.5 μm.

4) The total time t of the pulsed laser radiation action without taking into account the time of dark pauses (Table 2) (calculated by the formula $t = \tau \times f \times d/v$) [20], where τ is the duration of the laser light pulse (see Table 1), f is the frequency of the laser pulses, d is the diameter of the laser beam, v is the speed of the photographic plate, d/v is the time during which the photographic plate moved by the length of the laser beam diameter.

Table 2 – Total pulse time of femtosecond pulsed lasers

Laser name	Total pulse time, $t \times 10^{-5}$ s			
Flint	3,648 (Flint 1.0)	4,56 (Flint 2.0, Flint 4.0, Flint 6.0)		5,47 (Flint 10)
FemtoLux3	0.36	0.72	1.08	1.44	1.80

5) the number of quanta that fell on the volume of a conventional microcrystal with a size of 0.5 μm × 0.5 μm × 0.1 μm was determined through the proportion. For the lasers from Table 1, the values of σ_V were calculated using the method described in the work [20] (Table 3).

Table 3 – Calculated numerical values of σ_V of femtosecond pulsed lasers

Laser number from the Table 1	σ_V, $m^{-3} \cdot s^{-1}$	Laser number from the Table 1	σ_V, $m^{-3} \cdot s^{-1}$
1	1.21×10^{27}	6	0.9×10^{26}
2	3.02×10^{27}	7	1.8×10^{26}
3	6.05×10^{27}	8	2.7×10^{26}
4	9.08×10^{27}	9	3.56×10^{26}
5	18.16×10^{27}	10	4.46×10^{27}

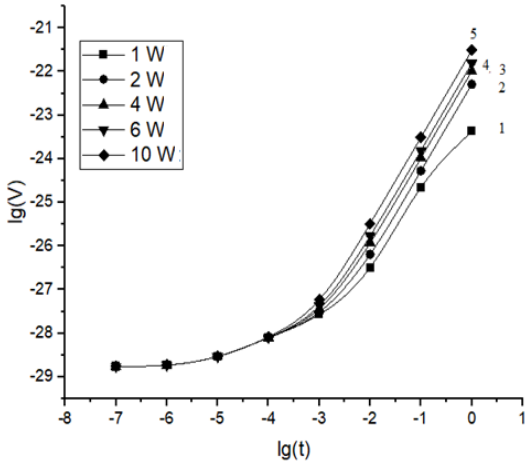

Fig. 1 – Growth kinetics on AgBr MC of Ag clots created by femtosecond pulsed lasers of the Flint series with $\lambda = 1035$ nm, frequency $f = 76$ MHz with different powers and durations of laser pulses according to the computer model. The number of each curve in Fig. 1 corresponds to the number of the Flint series laser from Table 1

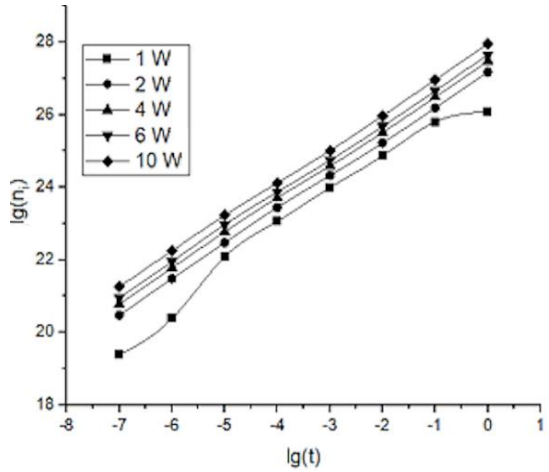

Fig. 2 – Kinetics of growth in AgBr MC of Ag ion concentration created by radiation of femtosecond pulsed lasers of the Flint series (Table 1) of different power according to the computer model. The number of each curve in Fig. 2 corresponds to the number of the Flint series laser from Table 1

Table 4 – Change in the volume of an Ag clot under the influence of radiation from Flint series lasers according to computer model data

Laser number from the Table 1	P (W)	$t = 10^{-7}$ s	$t = 10^{-6}$ s	$t = 10^{-5}$ s	$t = 10^{-4}$ s	$t = 10^{-3}$ s	$t = 10^{-2}$ s	$t = 10^{-1}$ s	$t = 1$ s
		$V \times 10^{-29}$, m^3				$V \times 10^{-28}$, m^3	V, m^3		
1	1	1.71	1.85	2.92	7.76	2.68	3.20×10^{-27}	2.20×10^{-25}	4.24×10^{-24}
2	2				7.80	3.05	6.42×10^{-27}	5.28×10^{-25}	5.10×10^{-23}
3	4			2.93	7.88	3.64	1.17×10^{-26}	1.04×10^{-24}	1.02×10^{-22}
4	6				7.96	4.22	1.70×10^{-26}	1.55×10^{-24}	1.55×10^{-22}
5	10				8.18	5.85	3.25×10^{-26}	3.09×10^{-24}	3.06×10^{-22}

Table 5 – Concentrations of silver ions (holes) ($n_i = n_h$ (m^{-3})) in AgBr MC at different times under the influence of radiation from Flint series femtosecond lasers according to computer model data

Laser number from the Table 1	P (W)	$t = 10^{-7}$ s	$t = 10^{-6}$ s	$t = 10^{-5}$ s	$t = 10^{-4}$ s	$t = 10^{-3}$ s	$t = 10^{-2}$ s	$t = 10^{-1}$ s	$t = 1$ s
		n_i, m^{-3}							
1	1	2.41×10^{19}	2.41×10^{20}	1.20×10^{22}	1.16×10^{23}	9.79×10^{23}	7.37×10^{24}	6.32×10^{25}	1.23×10^{26}
2	2	3.01×10^{20}	3.01×10^{21}	2.98×10^{22}	2.78×10^{23}	2.11×10^{24}	1.67×10^{25}	1.53×10^{26}	1.50×10^{26}
3	4	6.04×10^{20}	6.03×10^{21}	5.91×10^{22}	5.16×10^{23}	3.87×10^{24}	3.22×10^{25}	3.05×10^{26}	3.00×10^{27}
4	6	9.07×10^{20}	9.04×10^{21}	9.38×10^{22}	7.40×10^{23}	5.55×10^{24}	4.76×10^{25}	4.57×10^{26}	4.50×10^{27}
5	10	1.81×10^{21}	1.79×10^{22}	1.68×10^{23}	1.32×10^{23}	1.02×10^{25}	9.32×10^{25}	9.10×10^{26}	9.00×10^{27}

Table 6 – Change in the volume of an Ag clot under the influence of radiation from FemtoLux3 series lasers according to computer model data

Laser number from the table 1.	f. 10^6 s^{-1}	$t = 10^{-7}$ s	$t = 10^{-6}$ s	$t = 10^{-5}$ s	$t = 10^{-4}$ s	$t = 10^{-3}$ s	$t = 10^{-2}$ s	$t = 10^{-1}$ s	$t = 1$ s
		$V \times 10^{-29}$, m^3				$V \times 10^{-28}$, m^3	V, m^3	$V \times 10^{-26}$, m^3	$V \times 10^{-24}$, m^3
1	1	1.71	1.85	2.92	7.72	2.41	9.45×10^{-28}	1.91	1.56
2	2				7.73	2.43	1.11×10^{-27}	3.49	3.09
3	3					2.45	1.27×10^{-27}	5.05	4.61
4	4					2.47	1.43×10^{-27}	6.53	6.06
5	5				7.74	2.49	1.58×10^{-27}	8.08	7.58

The SDE (5) was solved using the fourth-order Runge-Kutta method.

3. RESULTS AND DISCUSSION

Using the computer model, the following results were obtained:

1) For the Flint series lasers:

The kinetics of Ag clot growth are shown in Fig. 1.

The values of the volume of Ag clusters on the AgBr MC calculated in the computer model at different times for pulsed femtosecond lasers of the Flint series are given in Table 4.

Fig. 2 shows the change in time in the AgBr MC of the Ag ion concentrations created by the radiation of the Flint series femtosecond pulsed lasers (see Table 1) according to the computer model.

The values of Ag ion concentrations in AgBr MC calculated in the computer model at different times for pulsed femtosecond lasers of the Flint series are given in Table 5.

2) For FemtoLux3 series lasers:

The kinetics of growth of Ag clots are given in Fig. 3.

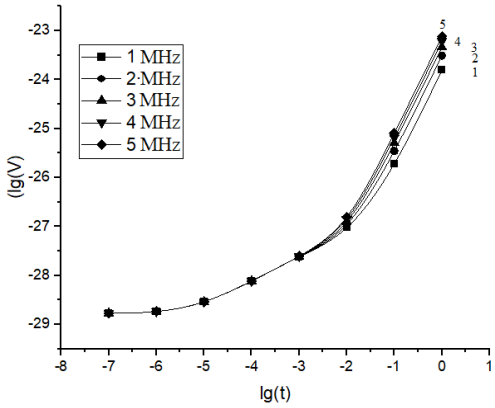

Fig. 3 – Growth kinetics in AgBr MC of Ag ions created by radiation of pulsed femtosecond lasers of the FemtoLux3 series for different pulse frequencies (Table 1) according to the data of the computer model. Curves 1, 2, 3, 4, 5 correspond to the parameters of lasers 6, 7, 8, 9, 10 from Table 1

Fig. 4 shows the changes in time in AgBr MC of Ag ion concentrations created by radiation of femtosecond pulsed lasers of the FemtoLux3 series (see Table 1) according to the data of the computer model.

Table 7 – Concentrations of silver ions (holes) $n_i = n_h$ (m^{-3}) in AgBr MC at different times under the action of radiation from femtosecond lasers of the FemtoLux3 series according to the data of the computer model

Laser number from the Table 1.	f. 10^6 s^{-1}	$t = 10^{-7}$ s	$t = 10^{-6}$ s	$t = 10^{-5}$ s	$t = 10^{-4}$ s	$t = 10^{-3}$ s	$t = 10^{-2}$ s	$t = 10^{-1}$ s	$t = 1$ s
		n_i, m^{-3}							
1	1	8.99×10^{18}	8.99×10^{19}	8.99×10^{20}	8.90×10^{21}	8.23×10^{22}	6.39×10^{23}	5.00×10^{24}	4.55×10^{25}
2	2	1.80×10^{19}	1.80×10^{20}	1.80×10^{21}	1.76×10^{22}	1.55×10^{23}	1.17×10^{24}	9.62×10^{24}	9.02×10^{25}
3	3	2.7×10^{19}	2.7×10^{20}	2.69×10^{21}	2.61×10^{22}	2.23×10^{23}	1.67×10^{24}	1.41×10^{25}	1.34×10^{26}
4	4	3.55×10^{19}	3.55×10^{20}	3.54×10^{21}	3.41×10^{22}	2.84×10^{23}	2.14×10^{24}	1.85×10^{25}	1.77×10^{26}
5	5	4.45×10^{19}	4.45×10^{20}	4.43×10^{21}	4.24×10^{22}	3.46×10^{23}	2.63×10^{24}	2.30×10^{25}	2.22×10^{26}

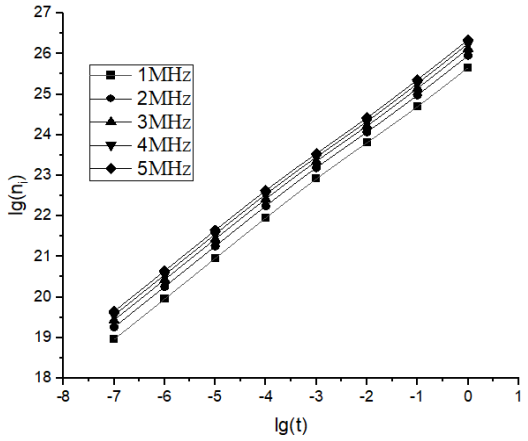

Fig. 4 – Kinetics of growth in the AgBr MC of the concentration of Ag ions created by the radiation of femtosecond pulsed lasers of the FemtoLux3 series (Table 1) of different pulse repetition rates according to the computer model. Curves 1, 2, 3, 4, 5 correspond to the parameters of lasers 6, 7, 8, 9, 10 from Table 1

The values of the volume of Ag clots on the AgBr MC calculated in the computer model at different times for the pulsed femtosecond lasers of the FemtoLux3 series are given in Table 6.

The values of the ion (hole) concentrations in the AgBr MC calculated in the computer model at different times for the pulsed femtosecond lasers of the FemtoLux3 series are given in Table 7.

Calculations in a computer model have established that under the action of the surface of the AgBr microcrystal radiation of a femtosecond pulsed laser with a wavelength of $\lambda = 1035$ nm and a constant frequency of $f = 76$ MHz of the Flint series, the growth time of the Ag clot to a volume of $V = 5.23 \times 10^{-26}$ m^3, at which its spontaneous crystallization is possible at room temperature, is:

a) $t = 4.74 \times 10^{-2}$·s for Flint 1.0 with a power of $P = 1$ W and a pulse duration of $\tau = 80 \times 10^{-15}$ s;

b) $t = 3.06 \times 10^{-2}$ s for Flint 2.0 with a power of $P = 2$ W and a pulse duration of $\tau = 100 \times 10^{-15}$ s;

c) $t = 2.18 \times 10^{-2}$ s for Flint 4.0 with power $P = 4$ W and pulse duration $\tau = 100 \times 10^{-15}$ s;

d) $t = 1.79 \times 10^{-2}$ s for Flint 6.0 with power $P = 6$ W and pulse duration $\tau = 100 \times 10^{-15}$ s;

e) $t = 1.27 \times 10^{-2}$ s for Flint 10 with power $P = 10$ W and pulse duration $\tau = 120 \times 10^{-15}$ s;

Therefore, increasing the power of the femtosecond laser and the pulse duration leads to a decrease in the growth time of the Ag clot to a volume $V = 5.23 \times 10^{-26}$ m^3. For the Flint 1.0, Flint 2.0, Flint 4.0, Flint 6.0, Flint 10 lasers, the growth time of an Ag clot to a volume of $V = 5.23 \times 10^{-26}$ m^3 is ~10^{-2} s. This is consistent with the fact that silver particles capable of being developed are not created during an exposure time of less than 10^{-5} s [25], and is also consistent with the basic provisions of the Chibisov-Galashin-Fock theory.

According to the computer model (Fig. 1, Table 4), in the time interval of $10^{-7} - 10^{-1}$ s of exposure to radiation from femtosecond pulsed lasers of the Flint series (Table 1) with a frequency of $f = 76$ MHz of different power, the volume of Ag clots on the surface of AgBr microcrystals increases from $V = 1.71 \times 10^{-29}$ m^3 to:

1. $V = 2.20 \times 10^{-25}$ m^3 for the Flint 1.0 laser with a power of 1 W and a pulse duration of $\tau = 80 \times 10^{-15}$ s.

2. $V = 5.28 \times 10^{-25}$ m^3 for the Flint 2.0 laser with a power of 2 W and a pulse duration of $\tau = 100 \times 10^{-15}$ s.

3. $V = 1.04 \times 10^{-24}$ m^3 for the Flint 4.0 laser with a power of 4 W and a pulse duration of $\tau = 100 \times 10^{-15}$ s.

4. $V = 1.55 \times 10^{-24}$ m^3 for the Flint 6.0 laser with a power of 6 W and a pulse duration of $\tau = 100 \times 10^{-15}$ s.

5. $V = 3.09 \times 10^{-24}$ m^3 for the Flint 10 laser with a power of 10 W and a pulse duration of $\tau = 120 \times 10^{-15}$ s.

Therefore, the Ag clot grows most rapidly when using the Flint 10 laser, which has the highest power and duration of the laser pulse at a constant frequency of $f = 76$ MHz among the used Flint series lasers. This occurs due to more intense heating of AgBr microcrystals by laser radiation and an increase in the concentration and mobility of Ag^+ ions and, as a result, a faster formation of Ag clots.

From Table 5 it follows that for a time $t = 10^{-7} - 10^{-1}$ s the concentration of Ag^+ ions increases within $n_i = 1.81 \times 10^{21} - 9.10 \times 10^{26}$m^{-3} for the Flint 10 laser with a power of 10 W and a laser pulse duration of $\tau = 120 \times 10^{-15}$ s. The value $n_i = 9.10 \times 10^{26}$ m^{-3} of the Ag^+ ion concentration is the largest value in Table 5 for a time $t = 10^{-1}$ s.

Also, calculations in the computer model established that under the action of the radiation of the FemtoLux3 series femtosecond pulse laser with a wavelength of $\lambda = 1030$ nm, power $P = 3$ W and laser pulse duration $\tau = 300 \times 10^{-15}$ s on the surface of the AgBr microcrystal, the growth time of the Ag clot to a volume of $V = 5.23 \times 10^{-26}$ m^3, at which its spontaneous crystallization is possible at a temperature of $T = 300$ K is:

a) $t = 1.72 \times 10^{-1}$ s for the laser pulse frequency $f = 1 \times 10^6$ s^{-1};

b) $t = 1.23 \times 10^{-1}$ s for the laser pulse frequency $f = 2 \times 10^6$ s^{-1};

c) $t = 1.018 \times 10^{-1}$ s for the laser pulse frequency $f = 3 \times 10^6$ s^{-1};

d) $t = 8.90 \times 10^{-2}$ s for the laser pulse frequency $f = 4 \times 10^6$ s^{-1};

e) $t = 7.97 \times 10^{-2}$ s for the laser pulse frequency $f = 5 \times 10^6$ s^{-1}.

Therefore, the growth time of an Ag clot to a volume $V = 5.23 \times 10^{-26}$ m^3 for FemtoLux3 series lasers is of the order of magnitude 10^{-2} s – 10^{-1} s. This is consistent with the fact that during an exposure time of less than 10^{-5} s, Ag particles capable of being developed are not created [25], and is also consistent with the basic provisions of the Chibisov-Galashin-Fock theory.

According to the computer model (Fig. 3, Table 6), in the time interval of $10^{-7} - 10^{-1}$ s of exposure to radiation of femtosecond pulsed lasers of the FemtoLux3 series (Table 1) with a wavelength of $\lambda = 1030$ nm, power $P = 3$ W and laser pulse duration $\tau = 300 \times 10^{-15}$ s, the volume of Ag clots on the surface of AgBr microcrystals increases from $V = 1.71 \times 10^{-29}$ m^3 to:

1. $V = 1.91 \times 10^{-26}$ m^3 for the laser pulse frequency $f = 1 \times 10^6$ s^{-1};

2. $V = 3.49 \times 10^{-26}$ m^3 for the laser pulse frequency $f = 2 \times 10^6$ s^{-1};

3. $V = 5.05 \times 10^{-26}$ m^3 for the laser pulse frequency $f = 3 \times 10^6$ s^{-1};

4. $V = 6.53 \times 10^{-26}$ m^3 for the laser pulse frequency $f = 4 \times 10^6$ s^{-1};

5. $V = 8.08 \times 10^{-26}$ m^3 for the laser pulse frequency $f = 5 \times 10^6$ s^{-1}.

So, among the used FemtoLux3 series lasers, the Ag clot grows the fastest in $10^{-7} - 10^{-1}$ s under the action of laser radiation with the highest laser pulse frequency $f = 5 \times 10^6$ s^{-1} at constant laser power and pulse duration. This occurs due to more intense heating of AgBr microcrystals by laser radiation and an increase in the concentration and mobility of Ag^+ ions and, as a result, faster formation of Ag clots.

From Table 7 it follows that for the time $t = 10^{-7} - 10^{-1}$ s the concentration of Ag^+ ions increases within the range $n_i = 4.45 \times 10^{19} - 2.30 \times 10^{25}$ m^{-3} for the FemtoLux3 series laser (Table 1) with a wavelength $\lambda = 1030$ nm, power $P = 3$ W, laser pulse duration $\tau = 300 \times 10^{-15}$ s and laser pulse frequency $f = 5 \times 10^6$ s^{-1}. The value $n_i = 2.30 \times 10^{25}$ m^{-3} of the Ag^+ ion concentration is the largest value in Table 7 for the time $t = 10^{-1}$ s.

4. CONCLUSIONS

1. It was established that under the action of the surface of the AgBr microcrystal by the radiation of a femtosecond pulsed laser with a wavelength of $\lambda = 1035$ nm and a constant frequency of $f = 76$ MHz of the Flint series, the growth time of the Ag clot to a volume of $V = 5.23 \times 10^{-26}$ m^{-3}, at which its spontaneous crystallization is possible at room temperature, is:

a) $t = 4.74 \times 10^{-2}$ s for Flint 1.0 with a power of $P = 1$ W and a pulse duration of $\tau = 80 \times 10^{-15}$ s;

b) $t = 3.06 \times 10^{-2}$ s for Flint 2.0 with a power of $P = 2$ W and a pulse duration of $\tau = 100 \times 10^{-15}$ s;

c) $t = 2.18 \times 10^{-2}$ s for Flint 4.0 with a power of $P = 4$ W and a pulse duration of $\tau = 100 \times 10^{-15}$ s;

d) $t = 1.79 \times 10^{-2}$ s for Flint 6.0 with a power of $P = 6$ W and a pulse duration of $\tau = 100 \times 10^{-15}$ s;

e) $t = 1.27 \times 10^{-2}$ s for Flint 10 with a power of $P = 10$ W and a pulse duration of $\tau = 120 \times 10^{-15}$ s.

Therefore, increasing the power of the FL and the pulse duration leads to a decrease in the growth time of the Ag clot to a volume $V = 5.23 \times 10^{-26}$ m^3. For the Flint 1.0, Flint 2.0, Flint 4.0, Flint 6.0, Flint 10 lasers, the growth time of the Ag clot to the volume $V = 5.23 \times 10^{-26}$ m^3 is ~ 10^{-2} s. This is consistent with the fact that during the exposure time of less than 10^{-5} s, silver particles capable of developing are not created [25], and is also consistent with the basic provisions of the Chibisov-Galashin-Fock theory.

2. It was established that under the action of the surface of the AgBr microcrystal by the radiation of the FemtoLux3 series femtosecond pulsed laser with a wavelength of $\lambda = 1030$ nm, power of $P = 3$ W and a constant laser pulse duration of $\tau = 300 \times 10^{-15}$ s, the growth time of the Ag clot to a volume of $V = 5.23 \times 10^{-26}$ m^3, at which its spontaneous crystallization at room temperature is possible, is:

a) $t = 1.72 \times 10^{-1}$ s for the laser pulse frequency $f = 1 \times 10^6$ s^{-1};

b) $t = 1.23 \times 10^{-1}$ s for the laser pulse frequency $f = 2 \times 10^6$ s^{-1};

c) $t = 1.018 \times 10^{-1}$ s for the laser pulse frequency $f = 3 \times 10^6$ s^{-1};

d) $t = 8.90 \times 10^{-2}$ s for the laser pulse frequency $f = 4 \times 10^6$ s^{-1};

e) $t = 7.97 \times 10^{-2}$ s for the laser pulse frequency $f = 5 \times 10^6$ s^{-1}.

Therefore, the growth time of the Ag clot to the volume $V = 5.23 \times 10^{-26}$ m^3 for FemtoLux3 series lasers is from ~ 10^{-2} s to ~ 10^{-1} s. This is consistent with the fact that during the exposure time of less than 10^{-5} s, Ag particles capable of developing are not created [25], and is also consistent with the main provisions of the Chibisov-Galashin-Fock theory.

3. From computer models for the Flint series lasers, it follows that with an increase in the power and pulse duration of the FL at a constant pulse repetition rate, the growth time of silver clots to a volume of $V = 5.23 \times 10^{-26}$ m^3 decreases.

4. From computer models for the FemtoLux3 series lasers, it follows that with an increase in the pulse repetition rate of the FL at constant power and pulse duration, the growth time of silver clots to a volume of $V = 5.23 \times 10^{-26}$ m^3 decreases.

REFERENCES

1. B. Guo, J. Sun, Y. Hua, et al., *Nanomanufacturing and Metrology* **3**, 26 (2020) https://doi.org/10.1007/s41871-020-00056-5.
2. *Terahertz, Ultrafast Lasers and their Medical and Industrial Applications* (Ed. by S. Wadi Harun) *IntechOpen*. **120**, (2022) https://doi.org/10.5772/intechopen.100712.
3. B. Guo, J. Sun, Y. Lu, L. Jiang, *Int. J. Extrem. Manuf.* **1**, 032004 (2019) https://doi.org/10.1088/2631-7990/ab3a24.
4. S. Wang, J. Yang, G. Deng, S. Zhou, *Materials* **17**, 557 (2024) https://doi.org/10.3390/ma17030557.
5. S.K. Sundaram, E. Mazur, *Nat. Mater.* **1**, 217 (2002) https://doi.org/10.1038/nmat767.
6. L. Jiang, A.D. Wang, B. Li, T.H. Cui, Y.F. Lu, *Light: Sci. Appl.* **7**, 17134 (2018) https://doi.org/10.1038/lsa.2017.134.
7. M. Malinauskas, A. Zukauskas, S. Hasegawa, et al., *Light Sci. Appl.* **5**, e16133 (2016) https://doi.org/10.1038/lsa.2016.133.
8. A.H. Zewail (Nobel Lecture). *Angew. Chem. Int. Ed.* **39**, 2586 (2000) https://doi.org/10.1002/1521-3773(20000804)39:15<2586::AID-ANIE2586>3.0.CO;2-O.
9. A.V. Khaneft, *Solid State Commun.* **362**, 115089 (2023) https://doi.org/10.1016/j.ssc.2023.115089.
10. S. Sharma, V. Dutta, P. Raizada, A. A. Hosseini-Bandegharaei, V.K. Thakur, S. Kalia, V.-H. Nguyen, P. Singh, *J. Environ. Chem. Eng.* **9**, 105157 (2021) https://doi.org/10.1016/j.jece.2021.105157.
11. H. Singh, K. Sharma, B. Honnappa, K. Sekar, T. Singh Kang, *Langmuir* **41** No 23, 14707 (2025) https://doi.org/10.1021/acs.langmuir.5c00379.
12. C.L. Riddle, D.M. Scates, R.G. Fronk, R.L. Demmer, P. Ghosh. *Pat.US* 20,250,020,815 A1, USA, publ. 2025.01.16
13. Z. Qinghai, W. Weiweng, Q. Yunlong, B. Mengqi, L. Rui, C. Guanghui, L. Chaojie, D. Jihai, *Micropor. Mesopor. Mater.* **389**, 113555 (2025) https://doi.org/10.1016/j.micromeso.2025.113555.
14. W. Chen, W. Wu, Q. Bai, J. Liu, C. Zheng, Q. Gao, F. Hu, Y. Zhang, T. Lu, *ACS Biomater. Sci. Eng.* **9** No 5, 2470 (2023) https://doi.org/10.1021/acsbiomaterials.3c00039.
15. M.Z.A. Warshagha, M. Muneer, *ACS Omega* **7** No 34, 30171 (2022) https://doi.org/10.1021/acsomega.2c03260.
16. K. Kumari, R. Chandra, S. Singh, *RSC Adv.* **15**, 17591 (2025) https://doi.org/10.1039/d5ra00336a.
17. Y. Chi, L. Zhao, X. Li, H. Zhu, W. Guo, *Appl. Surface Sci.* **440**, 907 (2018) https://doi.org/10.1016/j.apsusc.2018.01.248.
18. L. Cabral, E.R. Leite, E. Longo, M.A. San-Miguel, E.Z. da Silva, J. Andrés, *Nano Lett.* **24** No 10, 3021 (2024) https://doi.org/10.1021/acs.nanolett.3c04130.
19. A.B. Piven, O.B. Piven, Yu.M. Lopatkin, *J. Nano- Electron. Phys.* **5** No 1, 01028 (2013).
20. A.B. Piven, O.B. Piven, Yu.M. Lopatkin *J. Nano- Electron. Phys.* **3** No 4, 088 (2011).
21. O.B. Piven', A.M. Gusak, *Metallofizika* **14** No 12, 83 (1992)
22. L. Cabral, J. Andrés, E. Longo, M.A. San-Miguel, E.Z. da Silva, *Physchem.* **2** No 2, 179 (2022) https://doi.org/10.3390/physchem2020013.
23. J. Belloni, M. Treguer, H. Remita, Rene de Keyzer, *Nature* **402**, 865 (1999) https://doi.org/10.1038/47223.
24. T. Tani, *Photographic Sensitivity* (Oxford University Press: New York: 1995).
25. K.V. Chibisov, M.V. Fok, E.A. Galaschin, E.P. Senchenkov, *J. Phot. Sci.* **21** No 3, 125 (1973).

Кінетика росту згустків Ag на мікрокристалах AgBr під дією фемтосекундного імпульсного лазерного випромінювання

Олександр Б. Півень[1], Олег Б. Півень[2]

[1] *Черкаський державний технологічний університет, 18006 Черкаси, Україна*
[2] *Національний технічний університет України «Київський політехнічний інститут імені Ігоря Сікорського», 03056 Київ, Україна*

Комп'ютерним моделюванням виявлено кінетики росту згустків Ag до об'єму $V = 5.23 \times 10^{-26}$ м^3 на поверхні мікрокристалів AgBr фотоемульсії під дією фемтосекундного випромінювання імпульсних лазерів серії Flint (довжина хвилі $\lambda = 1035$ нм, частота слідування імпульсів $f = 76$ МГц), серії FemtoLux3 ($\lambda = 1030$ нм, потужність $P = 3$ Вт, тривалість імпульса $\tau = 300$ фс). Встановлено, що час росту згустків Ag на поверхні мікрокристалів AgBr до об'єму $V = 5.23 \times 10^{-26}$ м^3, при якому можлива спонтанна кристалізація згустків Ag при температурі $T = 300$ К становить 1) $\sim 10^{-1}$ с для лазерів серії FemtoLux3 ($f = 1$ МГц, 2 МГц, 3 МГц); 2) $\sim 10^{-2}$ с для лазерів Flint 1.0 ($P = 1$ Вт, $\tau = 80$ фс), Flint 2.0 ($P = 2$ Вт, $\tau = 100$ фс), Flint 4.0 ($P = 4$ Вт, $\tau = 100$ фс), Flint 6.0 ($P = 6$ Вт, $\tau = 100$ фс), Flint 10 ($P = 10$ Вт, $\tau = 120$ фс) і лазерів серії FemtoLux3 ($f = 4$ МГц, 5 МГц). Це узгоджується з тим, що за час експонування мікрокристалів AgBr, менший 10^{-5} с частинки Ag, здатні проявлятися, не створюються.

Ключові слова: Фемтосекундне лазерне випромінювання, Мікрокристал AgBr, Вплив лазерного випромінювання, Кінетика росту, Згусток срібла, Низькочутливий фотошар, Кристалізація.